JOURNAL OF MATERIALS SCIENCE 27 (1992) 5348–5356

Fabrication and microstructure–mechanical property relationships in Ce–TZPs

J. WANG
IRC in Materials for High Performance Applications, The University of Birmingham, Birmingham B15 2TT, UK

X. H. ZHENG
Department of Mechanical Engineering, Beijing Institute of Technology, Beijing, People's Republic of China

R. STEVENS
School of Materials, The University of Leeds, Leeds, UK

Ceria-stabilized tetragonal zirconia polycrystals(Ce–TZPs) have been fabricated via conventional sintering of commercially available electrofused and electrorefined CeO_2-doped ZrO_2 powder at 1550 °C for various periods from 0.5–30 h. The resultant grain sizes of the sintered materials were in the range 2–15 μm. The sintering of such electrorefined powder appears to occur by a liquid state sintering process, evinced in terms of the grain-size dependence on sintering time at 1550 °C and by direct TEM observation. The mechanical properties of the sintered materials have been characterized, including single-edge notch bend fracture toughness and three-point bend fracture strength. The grain-size dependence of these properties in the CeO_2-stabilized tetragonal polycrystals is very much different from that in Y_2O_3 stabilized tetragonal zirconia polycrystals (Y–TZPs). The transformation plasticity, which is represented by the yield stress behaviour and the total strain to fracture, plays an important role in the microstructure–property interrelationship in the Ce–TZPs.

1. Introduction

Transformation-toughened ceramics represent a class of structural ceramics with considerably enhanced mechanical and thermal properties [1, 2]. Among the toughened materials, tetragonal zirconia polycrystals (TZPs) offer the highest toughness values ever measured for ceramic materials. A fracture toughness value of $> 20\ MPa\ m^{0.5}$, which is comparable to that of cast iron, has been obtained in Ce–TZPs [3–5].

The highly improved mechanical properties in these transformation-toughened ceramics are related to the stress-induced transformation of the metastable tetragonal zirconia grains to the monoclinic phase at crack tip [6, 7]. Therefore, the transformability of the metastable tetragonal grains in the process zone plays a dominant role in the ultimate attainable properties of these materials. The microstructural and composition parameters, such as the type and content of stabilizer, grain size, grain morphology, matrix constraint, and grain-boundary phases, if any exist, will have a significant effect on the tetragonal to monoclinic transformation and therefore the mechanical properties. In terms of ceramic processing, TZPs are only obtainable in the ZrO_2–Y_2O_3 and ZrO_2–CeO_2 systems, via careful composition and microstructural control [3]. For example, Y–TZPs consist of tetragonal zirconia grains of 0.3–1.5 μm containing 2–3 mol % Y_2O_3 [8]; Ce–TZPs are composed of tetragonal zirconia grains containing 9–20 mol % CeO_2 [4, 9]. In Y–TZPs, both the fracture strength and fracture toughness increases almost linearly with increasing grain size from 0.5–1.5 μm, a consequence of the increased transformation zone size [8]. The relationship between the critical grain size at which the metastable tetragonal zirconia phase will spontaneously transform to the monoclinic phase on cooling from the sintering temperature and composition, is well established for the ZrO_2–Y_2O_3 system [5].

In contrast, a limited study has been made of the relationships between transformability and microstructural parameters in Ce–TZPs, although it has been widely appreciated that these materials exhibit a much improved fracture toughness over their Y_2O_3-stabilized counterparts. The critical grain size for the spontaneous tetragonal to monoclinic transformation in the CeO_2-stabilized zirconia ceramics is neither well defined nor well documented in published work [9]. Microstructurally, they often exhibit larger grain sizes than those stabilized with Y_2O_3 [10]. Their fracture strength is generally lower than that of the Y–TZPs, although they exhibit a much higher fracture toughness. It is very likely that the ultimate fracture strength of Ce–TZPs is controlled by the yield stress level which induces the tetragonal to monoclinic transformation. As has recently been established by Yu and Shetty [11, 12], and Reyes-Morel and co-workers [13,

0022–2461

14], the transformation zone in Ce–TZPs is much elongated and often ten times larger than that in Y–TZPs. However, the toughening efficiency associated with such large process zones is considerably reduced by the extended transformation plasticity [13, 14]. There is a dearth of information in the published work on the grain-size dependence of mechanical properties for Ce–TZPs, although materials of 0.5–5 μm in grain size had been fabricated and characterized by a few individual investigators [4, 11–14]. It is the objective of this work to present a systematic study of the fabrication, and microstructure–property relationships in Ce–TZPs.

2. Experimental procedure

The as-received zirconia powder doped with 12 mol % CeO_2 (Unitec Ceramic Ltd, Stafford, UK), which was electrofused and electrorefined, was compacted in a steel die of 45 mm diameter at a pressure of 32 MPa, followed by sintering at 1550 °C for various periods from 0.5–30 h (heating and cooling rates 3 °C min^{-1}), thus obtaining a wide grain-size range in the sintered specimens. Both the sintered density and grain size were measured for the sintered materials as a function of sintering time. The sintered density was measured using the water displacement method and grain size measurement was made using the standard line interception technique, when more than 200 grains were counted for each of the measurements. For mechanical property measurements, the sintered specimens were cut into bars of 2.5 mm × 3.5 mm × > 20 mm, which were then polished to 6 μm finish. Three-point bend tests were carried out using a span of 20 mm and cross-head speed of 0.5 mm min^{-1}. The fracture toughness of the specimens was measured using the three-point single-edge notch beam (SENB) technique (span 20 mm, cross-head speed 0.5 mm min^{-1}, notch width 400 μm). The Vickers indentation hardness was obtained using an indentation load of 50 kg. X-ray diffraction (XRD) phase analysis, SEM, and TEM were used to characterize the microstructure of the sintered materials.

3. Results and discussion

Fig. 1a–c show the sintered density and grain size as a function of sintering time at 1550 °C for the electrorefined ZrO_2 powder containing 12 mol % CeO_2. The sintered density appears to decrease sharply with increasing sintering time from 0.5–8 h, followed by a slight drop with further extended duration at 1550 °C. The relative density for the sample sintered at 1550 °C for 0.5 h was 99.20% theoretical density, compared with 97.29% theoretical density for the sample held for 30 h at the same temperature. As will be discussed, the decrease in the sintered density is due to the increased porosity level at grain boundaries/junctions associated with the grain coarsening, which is shown by the steady increase in grain size of the sintered materials at 1550 °C. Fig. 2 shows the Vickers hardness as a function of sintering time. The large decrease in the hardness is a result of grain coarsening and increasing porosity with increasing duration at 1550 °C.

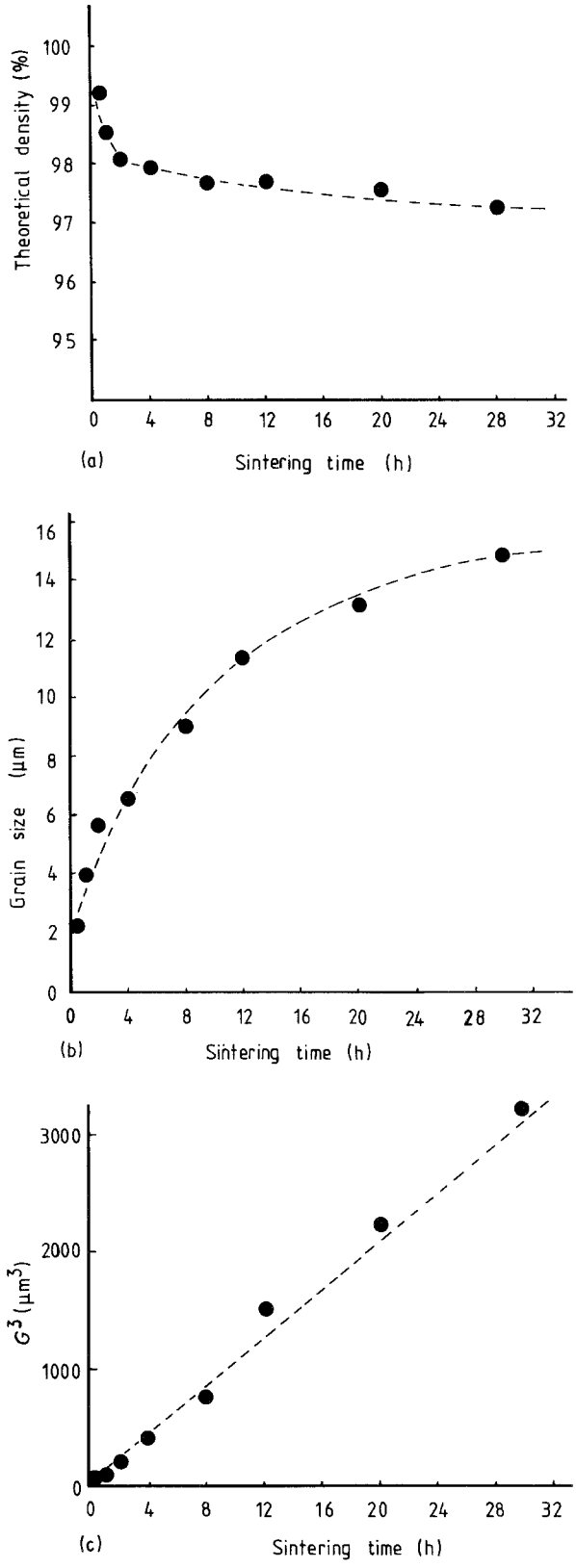

Figure 1 (a) The sintered density as a function of sintering time at 1550 °C, indicating that the sintered density decreases sharply with sintering time from 0.5–8 h. (b) The grain size as a function of sintering time at 1550 °C. The grain size appears initially to increase sharply with sintering time. The grain growth rate decreases steadily with increasing grain size. (c) The grain size (G)–sintering time (t) relationship at 1550 °C appears to fit approximately $G^3 \sim t$, which implies that the densification of the electrorefined ZrO_2 powder is via a liquid-assisted sintering process.

Using scanning electron microscopy, it was observed that only normal grain growth occurred when the electrorefined 12 mol % CeO_2-doped ZrO_2 powder was sintered at 1550 °C, Fig. 3a–f, which indicate a

TABLE I Impurities present in the as-received electrorefined ZrO_2 powder, indicating that silica is the principal impurity in the powder (wt %)

ZrO_2	HfO_2	CeO_2	SiO_2	CaO	Na_2O	K_2O	Al_2O_3	Fe_2O_3	MgO
81.72	1.70	16.05	0.16	0.04	< 0.1	< 0.01	0.13	0.09	< 0.05

narrow grain-size distribution for the materials sintered for various periods at 1550 °C. Detailed grain-size measurements showed that no significant change occurred in the standard deviation with increasing sintering time, although the average grain size increased steadily. As is widely accepted, the densification of commercially available ZrO_2 powders is often via a liquid state sintering process [15]. This is a consequence of the presence of a certain amount of silica/silicate impurities in most commercially available ZrO_2 powders, which are largely processed from zircon (zirconium silicate, $ZrSiO_4$). Table I shows that silica is the principal impurity present in the electrorefined CeO_2-doped ZrO_2 powder. It is therefore likely that its densification occurs via a liquid state sintering process. Two pieces of evidence were found in the present work to support this contention: the grain-size measurements and direct microstructural observation using transmission electron microscope (TEM).

As is indicated in Fig. 1c, the grain size(G)–time(t) relationship at 1550 °C appears to fit $G^3 \sim t$, which describes the normal grain growth in single-phase ceramics containing soluble impurities at grain boundaries [16, 17]. In comparison with the solid state sintering [18], the grain size(G)–time(t) relationship of which follows $G^2 \sim t$, the grain growth rate in materials involving a liquid phase at sintering temperatures decreases much more quickly with increasing grain size. We noted that the final sintered density of the electrorefined 12 mol % CeO_2-doped ZrO_2 powder (> 99% theoretical density) was much higher than that obtainable in some co-precipitated powders ZrO_2 powders. For example, the sintered density at 1550 °C/2 h for Toyo Soda 12Ce powder was < 96% theoretical density (12Ce is a 12 mol % CeO_2-doped ZrO_2 powder prepared using co-precipitation technique). The most noticeable difference in the impurity level between the electrorefined powder studied in this work and the Toyo Soda 12Ce powder is the silica content (0.16 wt % compared to 0.005 wt %). It can therefore be inferred that the improved sintered density of the electrorefined CeO_2-doped ZrO_2 powder is closely related to the high silica level present. The liquid silicate phases present at the grain boundaries and grain junctions assist the densification of this powder at the sintering temperature. Microstructural examination using transmission electron microscopy (TEM) confirmed the presence of a glassy phase at grain boundaries and grain junctions in the sintered materials, Fig. 4. Energy dispersive X-ray (EDX) phase analysis indicated that the glassy phase at the grain boundaries and grain junctions was silicon-rich.

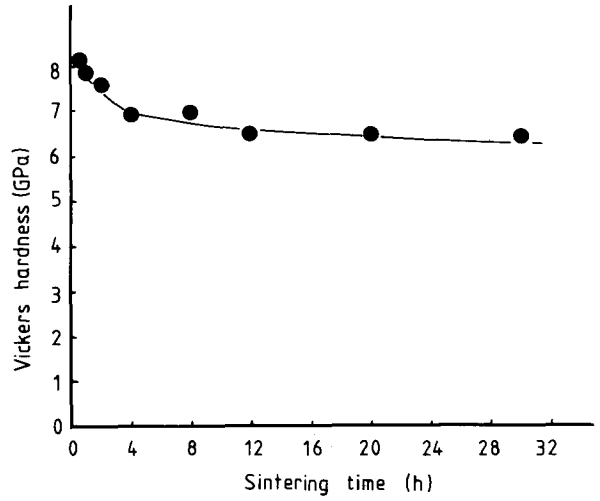

Figure 2 The Vickers hardness as a function of sintering time at 1550 °C. The large reduction in hardness with increasing sintering time from 0.5–8 h at 1550 °C is a result of grain coarsening and the increased porosity.

The grain size range (2–15 μm) obtained in the 12 mol % CeO_2-stabilized tetragonal zirconia polycrystals fabricated in this work is considerably wider than reported in the published work (0.5–5μm) [4, 11–14]. XRD phase analysis confirmed that the principal phase in all the materials sintered at 1550 °C was tetragonal, although there is a slight increase in the monoclinic phase content with increasing sintering time (the monoclinic phase content in the sample held for 30 h at 1550 °C was < 5%). Surface cracks were not observed even in the sample with grain size of 15 μm. Fine grain-sized materials (i.e. grain size < 1 μm) was not obtained in the present work, although experiments were conducted on sintering the electrorefined CeO_2-doped ZrO_2 powder at 1400 °C for 0.5 h. This was probably due to the relative large particle size of the starting powder (> 0.5 μm), Fig. 5. Ce–TZPs with grain sizes of 0.5 μm was fabricated using co-precipitated powders [9].

The principal difference in microstructure between Ce–TZPs and Y–TZPs is in their grain size [3]. The former tend to exhibit larger grain size than the latter. The critical grain sizes for Y–TZPs are generally limited to less than 2 μm, decreasing sharply with decreasing Y_2O_3 content [5]. In contrast, Ce–TZPs can, as is shown in the present work, have grain sizes of 15 μm. Therefore, they are much more tolerant of large grain size than Y–TZPs, in terms of the critical grain size for the spontaneous tetragonal to monoclinic transformation on cooling. As was noted by Duh *et al.* [10], a small addition of Y_2O_3 in Ce–TZPs resulted in an effective grain-size refinement.

Fig. 6 shows the SENB toughness as a function of grain size for the Ce–TZPs fabricated in this work. The SENB toughness appears to decrease dramatically with increasing grain size for the samples sintered for 0.5–8 h at 1550 °C, in a similar manner as the

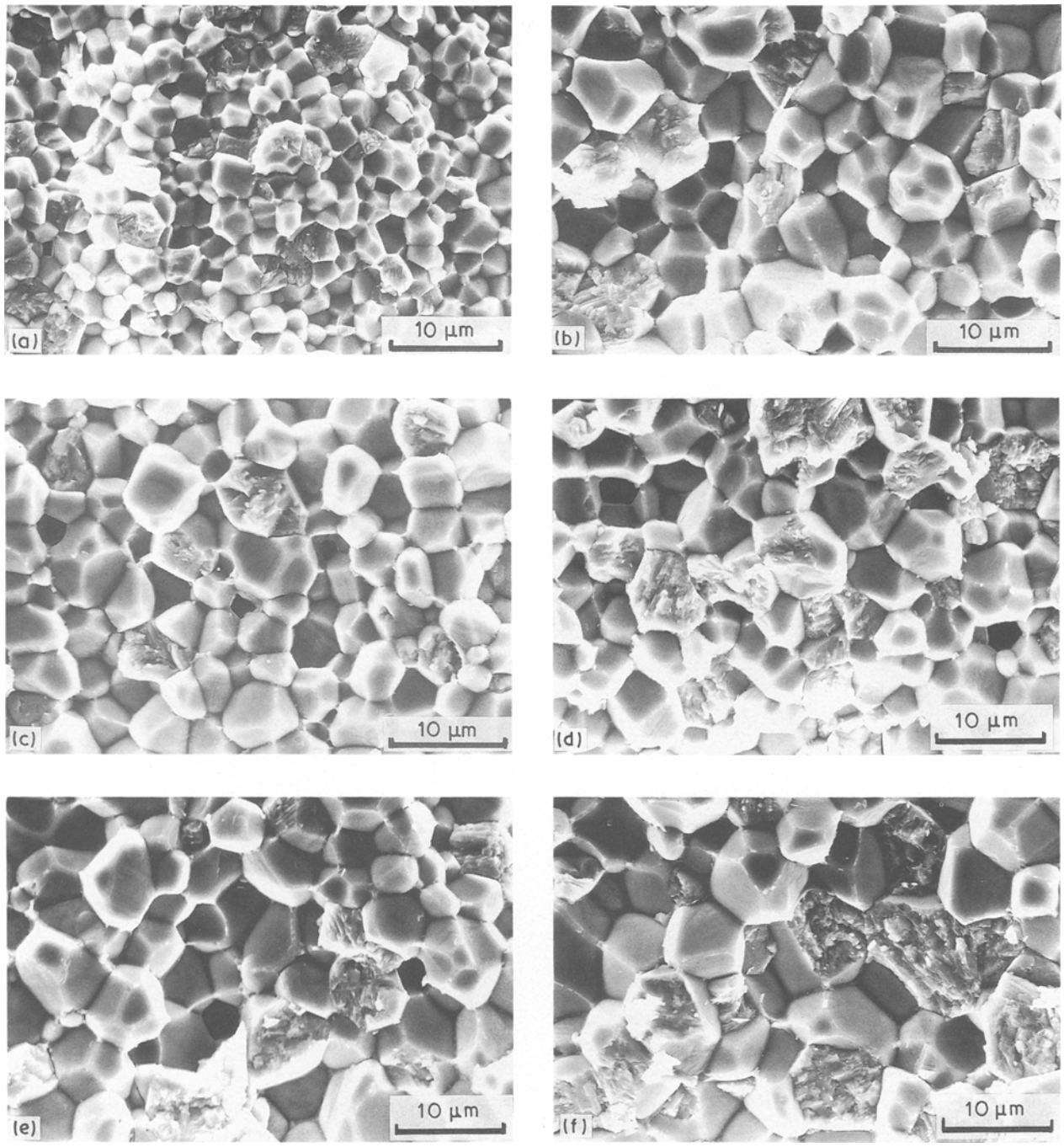

Figure 3 Scanning electron micrographs showing that (i) the grain size increases with increasing sintering time, and (ii) only normal grain growth occurs in the samples sintered at 1550 °C for various periods. (a) 2 h, (b) 4 h, (c) 8 h, (d) 12 h, (e) 20 h, (f) 30 h.

grain size dependence of the sintered density (indicated by Fig. 1a, b). This is significantly different from the mechanical property–grain size relationships in Y_2O_3 stabilized materials, in which a linear increase, followed by a fall in fracture toughness with increasing grain size, was observed [8]. It is a controversial fact that the larger grain-sized Ce–TZPs, which should exhibit an increased transformability and transformation zone size, show the reduced SENB toughness when compared with the finer grain-sized materials. Fig. 7 shows the three-point bend strength as a function of grain size for the same materials discussed in Fig. 6. In a similar manner to the SENB fracture toughness, the fracture strength appears to decrease sharply with increasing grain size for the samples sintered for 0.5–8 h. Further extended time at 1550 °C results in a minor reduction in the fracture strength. For Ce–TZPs, there exists two possible parameters which will eventually determine their fracture strength: namely, the yield stress for inducing the tetragonal to monoclinic transformation and the critical flaw size associated with microstructural imperfections. When one considers the relative small grain-size range of the materials fabricated in this work, it is unlikely that the largely decreased strength for 10–15 μm grain-sized materials is due to the increased flaw size associated with the increase in grain size. It is therefore speculated that the loss in the fracture strength is a result of the decreased yield stress of the large metastable tetragonal grains, which is thermodynamically more transformable.

It is well established that the stability of the

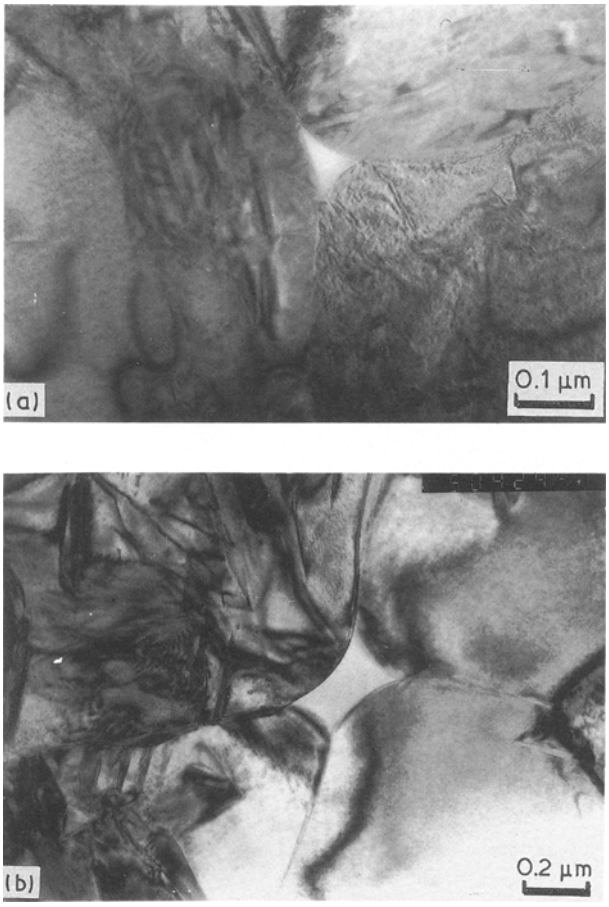

Figure 4 Two transmission electron micrographs showing the occurrence of a glassy phase at grain boundaries and junctions in the sintered material (8 h). The glassy phases are due to the high silica impurity in the electrorefined ZrO_2 powder. It is believed that the occurrence of such a liquid phase at sintering temperature assists the densification of zirconia ceramics. However, the resultant glassy phase at grain boundaries and junctions will suppress the autocatalytic nature of the transformation.

metastable tetragonal zirconia grains is affected by several microstructural and composition parameters including grain size and morphology, alloying type and content, and matrix constraint [2, 5, 19]. Grain size and alloying content (for a given alloying addition) are believed to be the two most determining

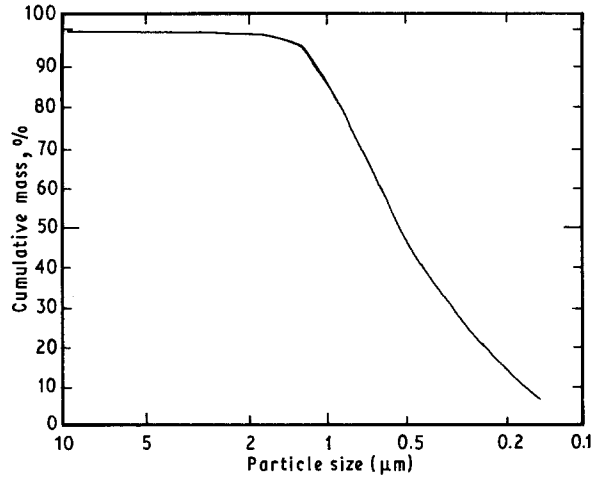

Figure 5 Particle size distribution in the as-received electrorefined ZrO_2 powder used in this work. The average particle size appears to be larger than that of co-precipitated ZrO_2 powders.

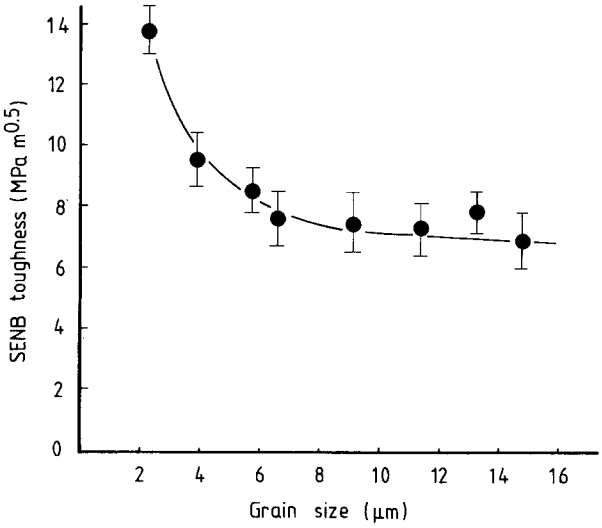

Figure 6 SENB toughness as a function of grain size for CeO_2-stabilized tetragonal zirconia polycrystals sintered at 1550 °C.

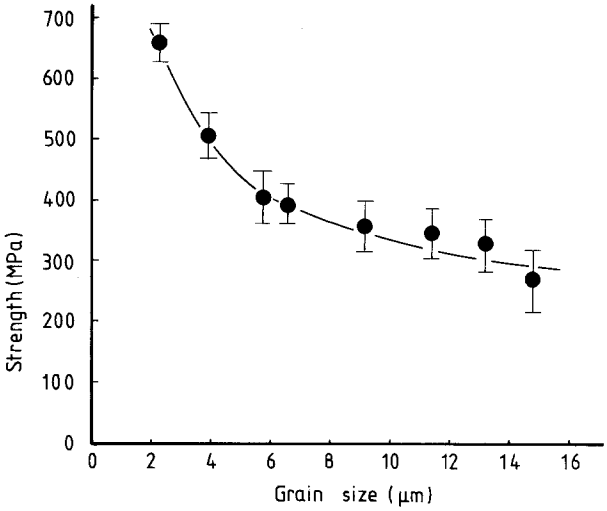

Figure 7 Three-point bend strength as a function of grain size for CeO_2-stabilized tetragonal zirconia polycrystals sintered at 1550 °C.

parameters among these known parameters. For a given composition, the mechanical properties (such as fracture toughness and fracture strength) of TZP ceramics will be largely dependent on the grain size of sintered materials. As was observed by Wang *et al.* [8], both the fracture toughness and fracture strength of Y–TZPs (containing 2, 2.5 and 3 mol % Y_2O_3, respectively) increase almost linearly with increasing grain size up to their critical grain sizes, where the spontaneous tetragonal to monoclinic transformation occurs on cooling from the sintering temperature.

As was pointed out above, it was unlikely that the flaw size in the Ce–TZPs fabricated in the present work was limited by the intrinsic faults, where the Griffith's law applies. It is therefore considered that the flaw size in these materials is governed by the transformation zone size, in which case the transformation stress is the controlling factor in determining their mechanical behaviour. On the basis of thermodynamics, it is known that the transformability of these metastable materials increases with an increase in grain size for a given composition [19]. Both

increasing stress (hydrostatic tension and/or shear) and decreasing temperature promote the transformation of the metastable tetragonal grains to the monoclinic phase, below the tetragonal to monoclinic equilibrium temperature [11, 12]. The ultimate fracture strength of these transformation-toughened ceramics is limited by the minimum stress which is required to induce the tetragonal to monoclinic transformation [7]. Therefore, the yield point on the stress–strain curve indicates the stress value at which the tetragonal to monoclinic transformation occurs. Thus, the yield stress can be regarded as a measure of the transformability of the metastable tetragonal phase. Reyes-Morel and co-workers [13, 14] and Yu and Shetty [11, 12] observed that the yield stress of 12 mol % Ce–TZPs decreases with increasing grain size in relatively small grain-sized materials (1.5–3.0 μm). As an example, a yield stress of 390 MPa for 1.47 μm grain-sized Ce–TZP containing 12 mol % CeO_2 is compared with a yield stress of 176 MPa for 2.18 μm grain-sized material containing the same amount of CeO_2.

Fig. 8 shows the yield stress of 12 mol % CeO_2 stabilized TZPs as a function of grain size in the grain size range 2–15 μm. The large grain-sized materials appear to exhibit lower yield stresses than those with small grain sizes. This inverse dependence of the transformation yield stress on the grain size can be regarded as a stress equivalence to the grain-size dependence of the starting transformation temperature, M_s, which decreases with increasing grain size, because the applied stress is introduced into the energy balance in terms of an interaction energy modifying the strain energy [2]. The discussion above may explain why highly toughened Ce–TZPs have relatively low fracture strength, in comparison with Y_2O_3-stabilized materials. It is noted that for similar grain sizes, the yield stress of the materials fabricated in the present work is much higher than that of the materials studied by Reyes-Morel and co-workers [13, 14], possibly due to the difference in their silicate impurity levels. The presence of a silicate layer at grain boundaries of the Ce–TZPs may result in a reduction in their transformability which is shown as an increase in their yield stresses, due to the stress relaxation at grain boundaries and the reduced autocatalytic effect.

Fig. 9 shows some examples of the stress–displacement curves for the Ce–TZPs fabricated in this work. In a simple sense, the displacement length of a three-point bend testing specimen can be regarded as a measure of strain under tensile stress. There are two

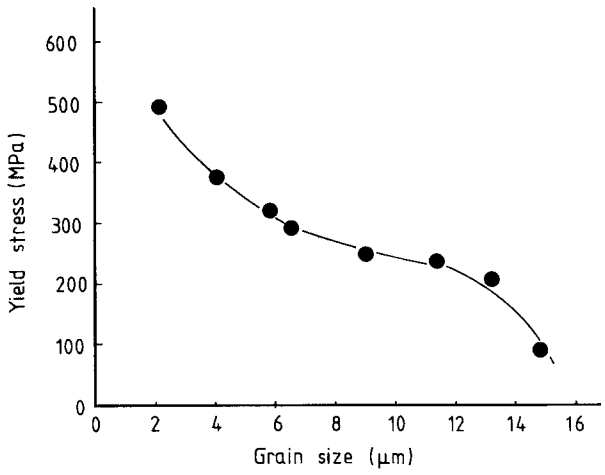

Figure 8 Grain-size dependence of the yield stress for CeO_2 stabilized tetragonal zirconia polycrystals sintered at 1550 °C.

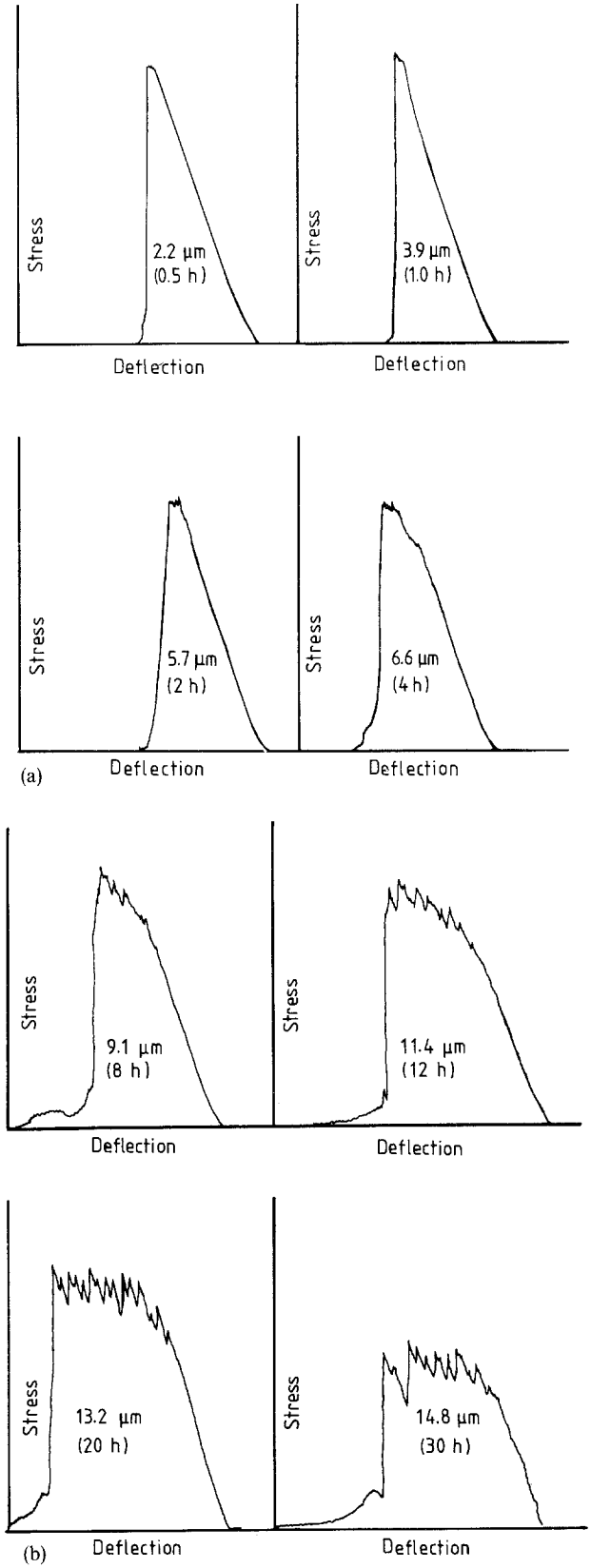

Figure 9 Three-point bend stress–displacement curves for CeO_2 stabilized tetragonal zirconia polycrystals exhibiting various grain sizes.

noticeable features which can be identified among the stress–displacement curves for the different grain-sized materials. The first interesting observation when the materials were subjected to three-point bend testing was the serrated flow shown on the stress–deflection curves above the yield stress. The serrated flow was also associated with the crack-like noise similar to "Tin Cry" when the materials were tested, indicating that it was due to the tetragonal to monoclinic transformation occurring on the tension surface of the specimens. Tsukuma and Shimada [4] and Reyes-Morel and co-workers [13, 14] noted the same phenomenon when they tested their CeO_2-stabilized materials. In particular, Tsukuma and Shimada [4] observed a very limited serrated flow in relatively small grain-sized materials (< 1 μm); Reyes-Morel and co-workers [13, 14], on the other hand, observed some extended serrated flow in 2.80 μm grain-sized material, indicating a grain-size dependence of the phenomenon in Ce–TZPs. It is believed that the sudden increase and decrease in stress was due to the discontinuity of the tension strain rate on the tensile surfaces, indicating the discrete nature of the transformation plasticity. Specifically, the serrated yielding is due to the occurrence of the tetragonal to monoclinic transformation in large and definite localized regions, i.e. the transformation of the metastable tetragonal grains ahead of a crack tip is not a continuous and homogeneous process, the grains subjected to a higher level of stress will transform prior to those subjected to a lower level of stress. For a given stress level, larger grains will undergo the tetragonal to monoclinic transformation prior to smaller grains. As will be discussed in the following sections, the occurrence of intergranular pores and glassy phase at grain boundaries and junctions in the coarse-grained materials may suppress the autocatalytic nature of the tetragonal to monoclinic transformation in the process zone. The grain-size dependence of the serrated flow shown in Fig. 9 implies that the transformation is a co-operative process only in localized regions, for the coarse-grained materials.

Ce–TZPs are the only transformation-toughened ceramics which are shown to exhibit such significant serrated flow in the stress–strain curve, although other similarly toughened materials (such as MgO and Y_2O_3 partially stabilized zirconia ceramics) exhibit some comparable fracture toughness values [11]. It is thus considered that the transformation characteristics in Ce–TZPs may be fundamentally different from those in MgO and Y_2O_3 partially stabilized zirconia ceramics. Discrete transformation bands analogous to Luders bands in steels have been found in Ce–TZPs when they were subjected to either compression or bending stresses [13]. In a three-point bend test, two transformation bands were observed to nucleate at the specimen edges on the tension surface, and propagate towards each other rapidly and join to form a single band whose length equalled the bend specimen width. More importantly, it has been demonstrated that the transformation zone shape, size and *R*-curve behaviour of Ce–TZPs are considerably different from those in MgO- and Y_2O_3-stabilized zirconia ceramics [11, 12]. The transformation zones in Ce–TZPs, which are thin elongated strips (of the order of hundreds of micrometres long) and resemble the plastic strip zones envisaged in the classic Dugdale model [20], are much larger and more elongated than those in MgO- and Y_2O_3-stabilized zirconia ceramics. They are, therefore, significantly different from the shapes predicated by the combined shear/dilatation yield criterion [2, 6]. As was observed by Yu and Shetty [11, 12], the length of the transformation zone at the crack tip in their 12 mol % CeO_2 stabilized TZPs could be extended up to 2 mm, compared with less than 100 μm observed in the MgO and Y_2O_3 partially stabilized zirconia, although the maximum fracture toughness values measured in these materials were comparable (14–15 MPa $m^{0.5}$). This suggests that the transformation zone in the Ce–TZPs is not as efficient in developing crack shielding via the compressive tractions at the zone boundary as those in the MgO- and Y_2O_3-stabilized zirconia ceramics. This infers that the crack shielding models based on the combined shear/dilatation yield criterion tend to overestimate the fracture toughness increments for Ce–TZPs in terms of the measured transformation zone size [2, 6].

Another interesting feature which can be identified in the stress–deflection (strain) curves is the grain-size dependence of the total strain to fracture, Figs 9 and 10. It is clearly demonstrated that the absolute strain to fracture beyond the yield point increases with increasing grain size. Yu and Shetty [11, 12] noted a similar phenomenon when they studied the transformation plasticity and *R*-curve behaviour for Ce–TZPs, i.e. the total strain to fracture increased with increasing grain size (from 0.22% for 1.47 μm grained material to 1.2% for 2.18 μm grained material). However, they failed to present a direct discussion on the relationship between total strain to fracture and the transformation characteristics, although it is apparent that the total strain is related to the transformation plasticity. In other words, the transformation plasticity in Ce–TZPs increases with increasing grain size.

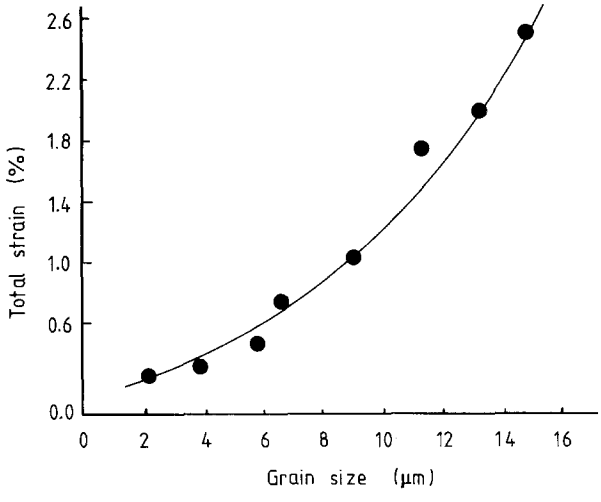

Figure 10 Grain-size dependence of total strain to fracture.

There are, for the Ce–TZPs, two factors which can help account for the observed grain-size dependence of mechanical properties and transformation plasticity: (i) the combined effects of phase transformation and damage in the process zone; (ii) the short-range autocatalytic and the long-range discrete nature of the transformation in the coarse-grained Ce–TZPs. As is shown in Figs 6 and 7, both the fracture toughness and fracture strength decrease with increasing grain size. This does not agree with the thermodynamic analysis which predicts that larger grains are more transformable than smaller grains and therefore should result in a more effective toughening. The irrelevent relationship between the transformation zone size and the toughness increment implies that there exists a counter-toughening process associated with the over-extended transformation zone (up to 2 mm) [11]. On considering that the tetragonal to monoclinic transformation is accompanied by a volume expansion and shear strain, it is speculated that a network of microcracks may well be induced in the largely transformed process zone. Rose and Swain [21], using scanning electron microscopy, noted intergranular microcracks in the transformation zone in Ce–TZPs. The presence of these microcracks in the process zone will result in a considerable damage both to the elastic properties and the resistance to fracture of these materials. As was observed by Evans and co-workers [2, 6], the fracture toughness of fully transformed monoclinic zirconia ceramics is less than 3 MPa $m^{0.5}$. Therefore, the toughening associated with the initial tetragonal to monoclinic transformation will almost immediately be offset by the resultant microcracks. The increased transformability of the coarse-grained materials will result in a higher density of microcracks in the process zone than in the fine-grained materials. Therefore, a more severe damage may be occurring in the process zone of the coarse-grained materials than in the fine-grained materials. This observation may be helpful in explaining the inverse relationships between the mechanical properties (SENB toughness and three-point bend strength) and grain size shown in Figs 6 and 7.

It has been suggested by Reyes-Morel and co-workers [7, 14] that the transformation in Ce–TZPs exhibits the autocatalytic nature, i.e. grains adjacent to an already transformed grain are favoured over other isolated grains for undergoing the tetragonal to monoclinic transformation. The volume and shear strains associated with the already transformed grain will assist the transformation of its neighbouring grains, in terms of the stress-induced nature of the transformation. However, such a co-operative process may become less and less important with increasing grain size. As is shown in Figs 1 and 2, there is a steady drop in the sintered density with increasing grain size. It was observed using scanning electron microscopy that the reduced sintered density was primarily due to the grain coarsening and the occurrence of angular pores at grain boundaries and junctions. It is considered that the voids at grain boundaries and junctions will greatly suppress the co-operative nature of the tetragonal to monoclinic transformation, as the volume and shear strains associated with a transforming grain will be automatically offset by the free space at the junctions with other grains. In a similar manner, the presence of a glassy silicate phase, the thickness of which increases with increasing grain size for a given amount of impurity level, at grain boundaries and junctions will also suppress the autocatalytic nature of the transformation. The counter-autocatalytic effects associated both with the intergranular porosity and with the grain-boundary glassy phase increase with increasing grain size. Microstructural examination using transmission electron microscopy (TEM) supports this consideration. It was observed that the tetragonal to monoclinic transformation in the thin foil specimen was often nucleated at angular regions which are adjacent to grain boundaries and grain junctions, Fig. 11. Similarly, MeCartney and Ruhle [22] also observed that the transformation usually started from the regions adjacent to grain junctions and grain boundaries in Y_2O_3-stabilized zirconia ceramics. Thermodynamically, the transformation is favoured to occur in these angular regions as they may be the areas of high free energy. Furthermore, stress concentration due to thermal mismatch and phase transformation is likely to occur in the regions adjacent to grain junctions. It is therefore easy to appreciate why the tetragonal to monoclinic transformation can be most effectively suppressed if voids and glass phases

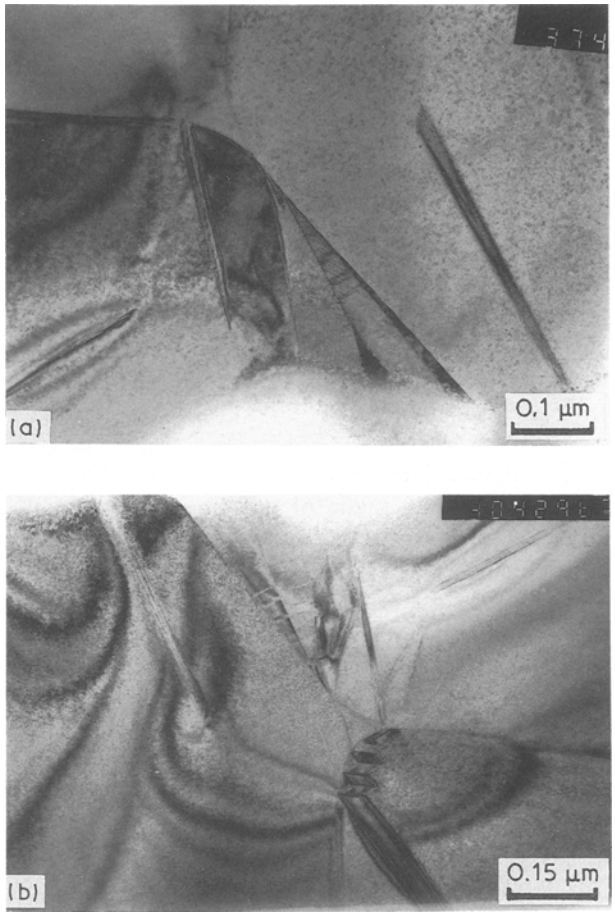

Figure 11 Transmission electron micrographs showing that the tetragonal to monoclinic transformation is often nucleated at grain boundaries and grain junctions in CeO_2 stabilized tetragonal zirconia polycrystals.

are present at grain boundaries and junctions in Ce–TZPs.

The above discussions do not conflict with the ideas of Chen and Chiao [23, 24], who believed that the tetragonal to monoclinic transformation in zirconia ceramics was nucleation controlled. The higher transformability of larger grain-sized materials over that of smaller grain-sized materials is a consequence of the increased possibility of nucleating the transformation. The superimposition of residual and externally applied stresses plays a dominant role in inducing the nucleation of the transformation. The autocatalytic nature of the transformation will be suppressed if there exists a space (i.e. either porosity or a glassy phase) isolating a transformed grain from its neighbours, although the transformability of an individual grain increases with increasing grain size. The presence of such intergranular discontinuities such as pores and a glassy phase layer at grain boundaries and junctions, in the coarse grain-sized materials, will be similar to the case when a non-transformable secondary phase is introduced into Ce–TZPs. Reyes-Morel and co-workers [13, 14] noted that the presence of alumina inclusions in Ce–TZPs resulted in a great reduction in the autocatalytic activity of the transformation in these materials. It should be pointed out that the autocatalytic nature of the transformation in Ce–TZPs may never be completely eliminated even when their sintered density is $< 97\%$ theoretical density. The grain-size dependence of the serrated flow shown in Fig. 9, indicates the occurrence of the autocatalytic transformation in certain localized regions, implying the short-range nature of the autocatalytically induced transformation in the coarse-grained materials. Each sudden drop and subsequent rise in stress is due to the strain release on the tensile surface, associated with the tetragonal to monoclinic transformation in a well-defined localized region. However, the interaction between different localized regions will become less and less apparent with increasing grain size. The increase in grain size will thus result in a suppression of the autocatalytic nature of the transformation in terms of the probability of long-range interactions.

4. Conclusions

A study has been made of the fabrication and the relationship between microstructure and mechanical properties in Ce–TZPs. As with most other zirconia ceramics, the densification of the electrorefined 12 mol % CeO_2-doped ZrO_2 powder appears to be a liquid-phase assisted sintering process. An extended sintering time at 1550 °C results in a reduction in the sintered density and grain coarsening. The microstructure–mechanical property relationships in Ce–TZPs are considerably different from those in Y_2O_3-stabilized zirconia ceramics in terms of the low transformation yield stress and high transformation plasticity. Both the fracture strength and fracture toughness decrease with increasing grain size for the composition containing 12 mol % CeO_2. The autocatalytic nature of the transformation can be largely suppressed by the grain coarsening, as a consequence of the occurrence of intergranular porosity and the increased thickness of glassy layers at grain boundaries and junctions.

Acknowledgement

The authors thank Simon Bradwell, School of Materials, The University of Leeds, for his assistance in preparing samples.

References

1. R. C. GARVIE, R. H. HANNINK and R. T. PASCOE, *Ceram. Steel, Nature (Lond.)* **258** (1975) 703.
2. A. G. EVANS and R. M. CANNON, *Acta Metall.* **34** (1986) 761.
3. I. NETTLESHIP and R. STEVENS, *Int. J. High Tech. Ceram.* **3** (1987) 1.
4. K. TSUKUMA and M. SHIMADA, *J. Mater. Sci.* **20** (1985) 1178.
5. F. F. LANGE, *ibid.* **17** (1982) 225.
6. R. McMEEKING and A. G. EVANS, *J. Amer. Ceram. Soc.* **65** (1982) 242.
7. I. W. CHEN and P. E. REYES-MOREL, *ibid.* **69** (1986) 181.
8. J. WANG, M. RAINFORTH and R. STEVENS, *Brit. Ceram. Trans. J.* **88** (1988) 1.
9. K. TSUKUMA, *Amer. Ceram. Soc. Bull.* **65** (1986) 1386.
10. J. G. DUH, H. T. DAI and B. S. CHIOU, *J. Amer. Ceram. Soc.* **71** (1988) 813.
11. C. S. YU and D. K. SHETTY, *J. Mater. Sci.* **25** (1990) 2025.
12. *Idem., J. Amer. Ceram. Soc.* **72** (1989) 921.
13. P. E. REYES-MOREL and I. W. CHEN, *ibid.* **71** (1988) 343.
14. P. E. REYES-MOREL, J. CHERNG and I. W. CHEN, *ibid.* **71** (1988) 648.
15. R. STEVENS, "An Introduction to Zirconia", 2nd Edn (MEL, Twickenham, 1986).
16. R. J. BROOK, *Scripta Metall.* **2** (1968) 375.
17. *Idem.*, in "Treatise on Materials Science and Technology", Vol. 2, edited by F. F. Y. Wang (Academic Press, New York, 1976) p. 331.
18. W. D. KINGERY, H. K. BOWEN and D. R. UHLMANN, "Introduction to Ceramics" (Wiley, New York, 1976).
19. R. C. GARVIE, *J. Phys. Chem.* **69** (1965) 1238.
20. D. S. DUGDALE, *J. Mech. Phys. Solids* **8** (1960) 100.
21. L. R. F. ROSE and M. V. SWAIN, *Acta Metall.* **36** (1988) 955.
22. M. L. McCARTNEY and M. RUHLE, *ibid.* **37** (1989) 1859.
23. I. W. CHEN and Y. H. CHIAO, *ibid.* **31** (1983) 10.
24. *Idem., ibid.* **33** (1985) 1827.

Received 17 June
and accepted 23 July 1991